Observation of Helicity-Induced Alfvén Eigenmodes in Large-Helical-Device Plasmas Heated by Neutral-Beam Injection

S. Yamamoto,[1] K. Toi,[2] N. Nakajima,[2] S. Ohdachi,[2] S. Sakakibara,[2] K. Y. Watanabe,[2] M. Goto,[2] K. Ikeda,[2] O. Kaneko,[2] K. Kawahata,[2] S. Masuzaki,[2] T. Morisaki,[2] S. Morita,[2] S. Murakami,[2] K. Narihara,[2] Y. Oka,[2] M. Osakabe,[2] Y. Takeiri,[2] K. Tanaka,[2] T. Tokuzawa,[2] K. Tsumori,[2] H. Yamada,[2] I. Yamada,[2] K. Yamazaki,[2] and LHD Experimental Group

[1]*Department of Energy Engineering and Science, Nagoya University, Nagoya-shi 464-01, Japan.*

[2]*National Institute for Fusion Science, Toki-shi 509-5292, Japan*

(Received 6 May 2003; published 9 December 2003)

The helicity-induced Alfvén eigenmodes (HAEs) with the toroidal mode number $n = 2$ and 3 are observed for the first time in the Large Helical Device plasmas heated by neutral beam injection. The observed mode frequency is about 8 times higher than that of the observed toroidicity-induced Alfvén eigenmodes, and is proportional to the Alfvén velocity. The modes are excited when the ratio of the beam velocity to the Alfvén velocity exceeds about unity. The frequency lies just above the lower bound of the HAE gap in the plasma edge region of $\rho > 0.7$ (ρ: normalized minor radius).

DOI: 10.1103/PhysRevLett.91.245001 PACS numbers: 52.35.Bj, 52.55.Hc, 52.55.Pi

In a deuterium-tritium (D-T) fusion reactor such as the International Thermonuclear Experimental Reactor, the Alfvén eigenmodes (AEs) destabilized by the alpha particles may quench the fusion burn and damage the first wall of a reactor because of significant loss of alpha particles from the confinement region before the thermalization. Therefore, the AEs are extensively being studied from various aspects in many tokamaks and helical devices using the energetic ions produced by neutral-beam injection (NBI), ion cyclotron resonance heating, and D-T reaction [1]. Moreover, the AEs would give important information about MHD spectra [2], and have a connection with a direct energy channeling of alpha particles to the bulk plasma [3]. For these reasons, AEs are of great importance in basic plasma physics as well as nuclear fusion research.

One of the most important AEs is toroidicity-induced Alfvén eigenmodes (TAEs) [4], which are generally the most unstable AEs in a tokamak plasma. The TAEs exist in the lowest shear Alfvén spectrum gaps formed by poloidal mode coupling between m and $m + 1$ Fourier modes due to the toroidal effect. The other spectrum gaps can be generated by higher order nonuniformity in the poloidal direction on the magnetic surface such as the ellipticity and noncircular triangularity [5]. They are ellipticity-induced AEs (EAEs) and noncircular triangularity-induced AEs (NAEs). These AEs are observed in many tokamaks [1]. In particular, TAEs do enhance energetic ion transport [1]. Moreover, TAEs are also detected in three-dimensional (3D) plasmas with the finite magnetic shear of the Compact Helical System (CHS) [6,7] and the Large Helical Device (LHD) [7,8]. In these cases, the TAE gap structure can be analyzed by the two-dimensional (2D) configuration where the poloidal mode coupling is essential. In the three-dimensional configuration where the magnetic field strength varies in both poloidal and toroidal directions on each magnetic surface, the toroidal mode coupling as well as poloidal mode coupling plays an important role in generating a new shear Alfvén spectrum gap. The helicity-induced Alfvén eigenmodes (HAEs) [9–11] can be excited inside the new gap generated by helical field components of the confinement magnetic field.

For a general description of AEs, we introduce a model confinement magnetic field with the field period number N_p, of which strength is expressed as

$$B = B_0 h, \qquad h = 1 + \sum_{\mu,\nu} \varepsilon_B^{(\mu,\nu)}(\psi) \cos(\mu\theta - \nu N_p \phi), \tag{1}$$

where ψ, θ, and ϕ are the toroidal magnetic flux, the poloidal and toroidal angles, and μ and ν are integers. The AE gap in this field is given by the following equation:

$$f_{\mathrm{AE}}^{(\mu,\nu)}(\iota) = |N_p \nu - \mu \iota_*| \frac{v_A}{4\pi R}. \tag{2}$$

Here, $v_A = B_t/(\mu_0 \rho_m)^{1/2}$ is the Alfvén velocity, B_t the magnetic field, ρ_m the ion mass density, and R the plasma major radius. The rotational transform ι_* is obtained from the intersection point of two Alfvén continua related to $\cos(\mu\theta - \nu N_p \phi)$ and $\cos[(m + \mu)\theta - (n + \nu N_p)\phi]$ Fourier modes; that is,

$$\iota_* = \frac{2n + \nu N_p}{2m + \mu}. \tag{3}$$

Moreover, the resonant condition for HAE is expressed as

$$v_{b\parallel}/v_A > \left(1 \mp \frac{2\iota_*}{N_p \nu - \mu \iota_*}\right)^{-1}, \tag{4}$$

where $v_{b\parallel}$ is energetic ion velocity.

In these equations, TAE, EAE, and NAE, respectively, correspond to the case of ($\mu = 1$, $\nu = 0$), ($\mu = 2$, $\nu = 0$),

and ($\mu = 3$, $\nu = 0$), and are related to the variation of the field strength as $\cos\theta$, $\cos 2\theta$, and $\cos 3\theta$. The HAE for the case of $\mu = 2$ and $\nu = 1$ is related to the variation of the field strength as $\cos(2\theta - N_p\phi)$. As seen from Eq. (2), HAE with $\mu = 2$ and $\nu = 1$ has higher frequency by a factor of about N_p/ι_* compared with the TAE gap frequency. In LHD, which is a heliotron- or torsatron-type device with $N_p = 10$ [12], the HAE gap frequency is considerably higher than the TAE frequency. The spectrum gap is fairly large because the gap width is proportional to the HAE gap frequency. It should be noted that HAE may be crucial for an advanced stellarator with small N_p such as the Wendelstein 7-X (W7-X) with $N_p = 5$ [13], National Compact Stellarator Experiment (NCSX) with $N_p = 3$ [14], and Quasiaxisymmetric CHS (CHS-QA) with $N_p = 2$ [15], because the HAE gap frequency in these configurations becomes comparable or less than the TAE gap frequency [11]. The linear growth rate of AE γ_L is typically expressed as

$$\gamma_L \propto \langle \beta_{b\parallel} \rangle \left(\frac{\omega_{*i}}{\omega_r} - \frac{1}{2} \right) F(v_{b\parallel}/v_A), \tag{5}$$

when the energetic ion has a slowing-down energy distribution, where $\langle \beta_{b\parallel} \rangle$, ω_{*i}, ω_r, and $F(v_{b\parallel}/v_A)$ are the averaged beta value of energetic ions, diamagnetic drift frequency of energetic ions, mode frequency of AE, and the fraction of resonant particles, respectively. As seen from Eq. (5), AEs become unstable when the condition of $\omega_r < 2\omega_{*i}$ is satisfied. The lower the mode frequency ω_r, the larger the growth rate becomes. Therefore, AEs with lower frequency are thought to be more dangerous.

The LHD [12] is the $l = 2$ heliotron- or torsatron-type device with $N_p = 10$, of which typical major and averaged minor radii are $R \sim 3.6$ m and $\langle a \rangle \sim 0.6$ m, respectively. In LHD, the magnetic axis position $R_{\rm ax}$ defined in the vacuum magnetic field, net plasma current, and the averaged plasma beta considerably modify the shear Alfvén spectrum due to the change of the rotational transform profile. The rotational transform in a low beta plasma decreases toward the plasma edge in contrast with a standard tokamak configuration. The shear Alfvén spectrum in LHD exhibits different characters for those in tokamaks.

MHD fluctuations are measured by magnetic probe arrays that have frequency response up to 600 kHz. The toroidal mode number n and poloidal mode number m are determined by a toroidal array of six probes and a helical array of 12 probes, which are arranged inside the vacuum vessel along the helical coil of LHD. The toroidal and poloidal mode numbers are successfully determined in the range of $|n| \leq 5$ and $|m| \leq 7$ by using these probe arrays. The magnetic probe signals are acquired with 500 kHz sampling rate in most cases, and are filtered with a low pass filter of 250 kHz cutoff frequency to avoid an alias effect.

The MHD instabilities with $n = 2$ and 3, of which frequencies are about 8 times higher than that of the observed TAE, are newly observed in NBI-heated plasmas of LHD at low magnetic field ($B_t < 0.7$ T). A typical discharge where the high frequency mode with $n = 2$ is observed is shown in Fig. 1. In this shot, hydrogen beams with the energy of $E_{\rm NBI} \sim 150$ keV and the power of $P_{\rm NBI} \sim 3$ MW are tangentially coinjected and counterinjected into a hydrogen plasma in the configuration of $R_{\rm ax} = 3.6$ m at $B_t = 0.5$ T. Bursting $n = 2$ TAEs with $m \sim 3$ and $n = 0$ global Alfvén eigenmodes (GAEs) are excited when a plasma is successfully produced by NBI alone. The energetic ion transport is appreciably affected by the bursting TAEs with large amplitude. In this phase, the velocity of beam ion exceeds the Alfvén velocity, and the excitation conditions for TAE and GAE are already satisfied. The high frequency mode with $n = 2$, of which frequency is in the range of $180 < f_{\rm exp} < 230$ kHz, is excited after $t \sim 1$ s. The high frequency mode propagates in the diamagnetic drift direction of energetic ions. The magnetic fluctuation amplitude of the high frequency

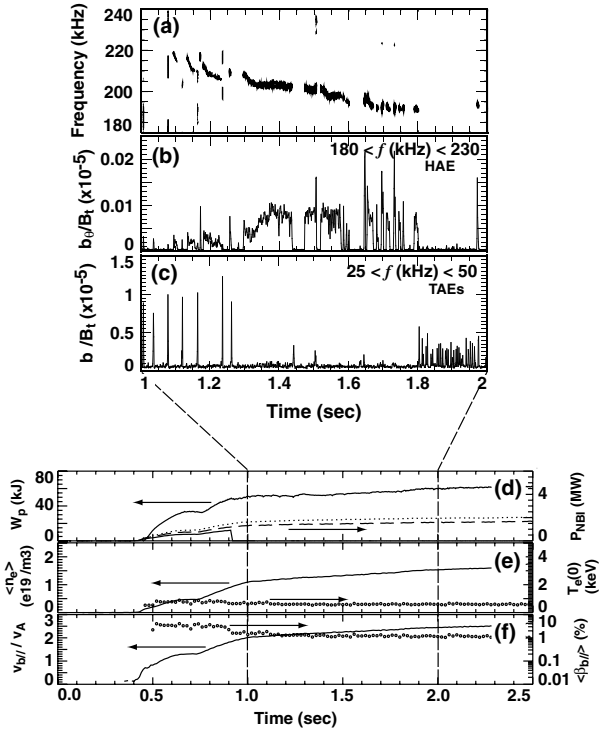

FIG. 1. (a) Time evolution of the magnetic fluctuations in an NBI-heated hydrogen plasma at low magnetic field $B_t = 0.5$ T in $R_{\rm ax} = 3.6$ m configuration where the high frequency mode with $n = 2$ is destabilized by energetic ions, (b) bandpass filtered ($180 < f < 230$ kHz) magnetic fluctuation including high frequency modes, (c) bandpass filtered ($25 < f < 50$ kHz) magnetic fluctuation including TAEs. (d) Time evolution of the plasma stored energy W_p and absorbed NBI power $P_{\rm NBI}$, where $P_{\rm NBI} \sim 3.8$ MW. (e) Time evolution of the line averaged electron density $\langle n_e \rangle$ and electron temperature at the plasma center $T_e(0)$, and (f) the ratio of $v_{b\parallel}/v_A$ and averaged beam beta $\langle \beta_{b\parallel} \rangle$ estimated on the assumption of classical slowing down.

mode is on the order of $b_\theta/B_t \sim 10^{-7}$ at the probe position, which is 2 orders of magnitude smaller than that of TAEs. It should be noted that the high frequency modes are interrupted by the bursting TAEs shown in Figs. 1(b) and 1(c).

The frequencies of high frequency modes with $n = 2$ and 3 are proportional to the Alfvén velocity as shown in Fig. 2, so that the high frequency mode is not be a beam mode such as energetic particle mode, of which frequency is determined by energetic ion velocity. The frequency of high frequency modes with $n = 3$, which are observed in a few shots, is by about 20% higher than that of high frequency modes with $n = 2$. Note that the Doppler shift for these $n = 2$ and $n = 3$ modes can be neglected because of very low toroidal plasma rotation.

In order to identify these observed modes, we compare the observed frequency at $t = 1.4$ s in the plasma shown in Fig. 1 with the shear Alfvén spectrum calculated for three-dimensional magnetic configuration, where poloidal and toroidal mode coupling are taken into account. The number of mode family is given by $1 + (N_p/2)$ [16], so that six mode families for LHD of $N_p = 10$ should be taken into account in the calculation of the shear Alfvén spectra. A family of modes with toroidal mode number n' satisfying the relation $n' \pm n = kN_p$ ($k = \ldots, -2, -1, 0, 1, 2, \ldots$) can couple with the mode having the toroidal mode number n [17]. In LHD, for instance, the $N_f = 2$ mode family which can couple with $n = 2$ mode is composed by Fourier modes with $n' = \pm 2, \pm 8, \pm 12, \pm 18$, etc. Thus calculated spectra are shown in Fig. 3. The gap structures are produced through poloidal and toroidal mode coupling for all Fourier modes with different toroidal mode number in the same mode family, where 919 Fourier modes with $n = 2$–52 are taken into account. In the calculation of this shear Alfvén spectrum, the plasma equilibrium is calculated by the VMEC code using Thomson scattering and far-infrared–-interferometer data. The pressure profile of energetic ions $P_{b\|}(\rho)$ is assumed to be $P_{b\|}(\rho) = P_{b\|}(0)(1 - \rho^8)^2$. The Shafranov shift of the plasma equilibrium calculated including $P_{b\|}(\rho)$ is consistent with the experimental data obtained from Thomson scattering and soft x-ray array data. The lowest spectrum gap is TAE gap having the good alignment from the plasma core towards the edge because of large Shafranov shift and the reduced magnetic shear in such high beta case of $\langle\beta_{\rm bulk}\rangle \sim 1.5\%$ ($\langle\beta_{\rm bulk}\rangle$: averaged toroidal beta of the bulk plasma). The HAE gap at the plasma center is in the higher frequency range of 350 to 600 kHz, and in the range of ~100 to ~700 kHz in the edge region. The continua with high-n mode ($n = 52$) remain inside the HAE gap because only a finite number of Fourier modes are taken into account. Moreover, new

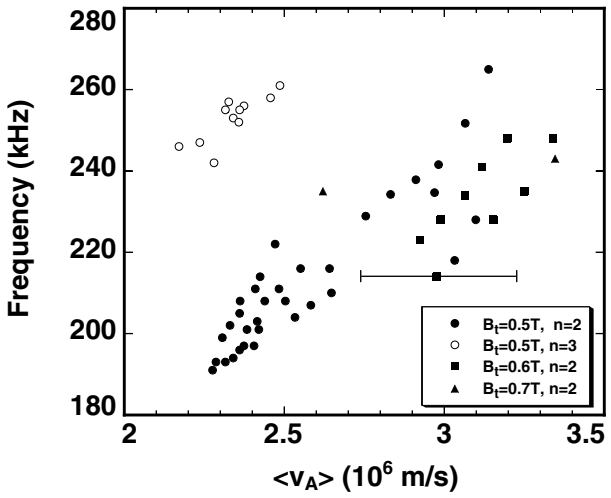

FIG. 2. Dependence of the observed frequency of high frequency modes with $n = 2$ and 3 on the Alfvén velocity $\langle v_A\rangle$ estimated using the line averaged density $\langle n_e\rangle$.

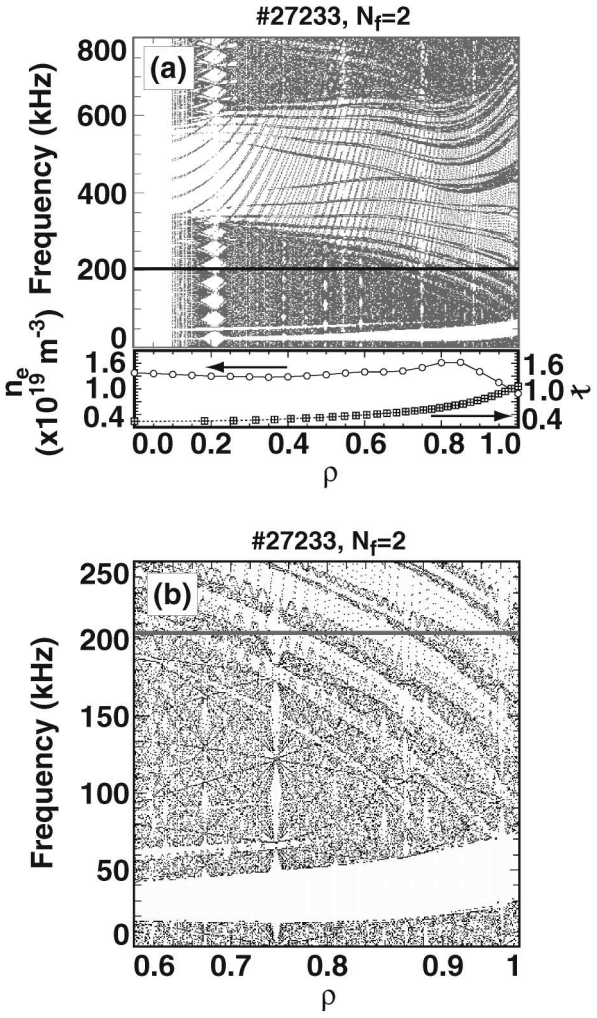

FIG. 3. (a) Calculated shear Alfvén spectra at $t = 1.4$ s of the plasma shown in Fig. 1, where 919 Fourier modes $n = 2, 8, \ldots, 48, 52$ are taken into account. The profiles of electron density and rotational transform in the lower trace are employed for the calculation. (b) Expanded view of Fig. 3(a). The solid lines in Figs. 3(a) and 3(b) indicate the observed frequencies ($f_{\rm exp} = 203$ kHz).

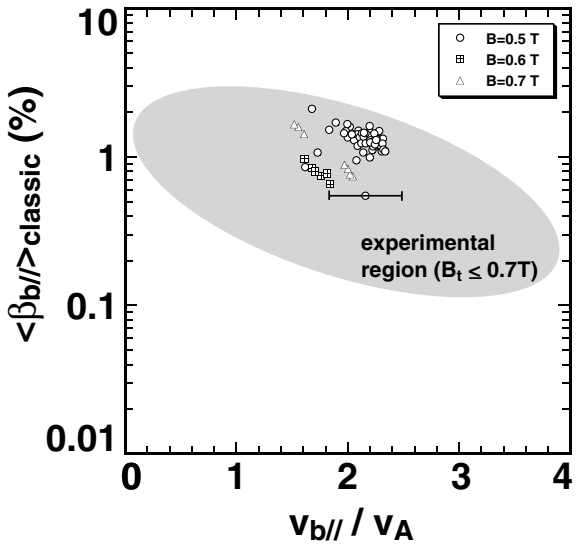

FIG. 4. Data points of the observed HAEs with $n = 2$ and 3 plotted on the parameter space defined by the ratio of $v_{b\|}/v_A$ and the beam beta $\langle\beta_{b\|}\rangle$. The gray hatched region indicates the range scanned experimentally in the plasma condition of $B_t < 0.7$ T and $R_{ax} = 3.6$ m.

continua inside HAE gap are generated by the lack of helical symmetry of helical field components and are thought to be related to discrete modes. The gray solid line in Fig. 3 indicates the measured frequency of the high frequency mode. The frequency lies in the HAE gap in the plasma edge ($\rho > 0.7$) and intersects with the lower bound of HAE more inside the region. Moreover, the frequency intersects with above-mentioned continua inside the HAE gap in the edge region. The profile of energetic ion pressure is thought to be fairly broad because the Larmor radius of passing energetic ions reaches up to 10% of plasma minor radius. Therefore, the gradient of energetic ion pressure has a peak near the plasma edge and energetic ion drive of the mode may be significantly large enough to overcome the continuum damping in the edge region. It is speculated that the observed high frequency modes are related to the HAE localized in the edge gap region. This seems to be consistent with the fact that the HAE fluctuations are interrupted by $m \sim 3/n = 2$ bursting TAE excited in the edge region around $\rho \sim 0.7$.

The excitation condition of AEs would depend on the average beam beta $\langle\beta_{b\|}\rangle$ and the resonance condition between energetic ions and Alfvén waves expressed by Eq. (4). The $\langle\beta_{b\|}\rangle$ is estimated as $\langle\beta_{b_\|}\rangle = \tau_s\langle\beta_{\rm bulk}\rangle/\tau_E$ on the assumption of the classical energy slowing down, where τ_s and τ_E are, respectively, the classical energy slowing-down time and global energy confinement time. In this estimation, energetic ion loss such as orbit loss, charge exchange loss, and MHD instability-induced losses are ignored. Therefore, $\langle\beta_{b||}\rangle$ is the upper bound of an actual value. The excitation condition of $n = 2$ HAEs is investigated on the parameter space shown in Fig. 4. The $n = 2$ HAEs are destabilized in the range of $\langle\beta_{b||}\rangle \geq 1\%$ and $1.5 \leq v_{b\|}/v_A \leq 2.4$. This range of $v_{b\|}/v_A$ is consistent with the fundamental excitation of HAE with $n = 2$ and $4 < m < 13$ ($1.4 > \iota_* > 0.5$).

In summary, the $n = 2$ and 3 high frequency modes, of which frequencies are about 8 times higher than that of the observed TAEs with $m \sim 3/n = 2$, are observed in NBI-heated LHD plasmas in the condition of $R_{ax} = 3.6$ m and $B_t \leq 0.7$ T. The frequencies of the high frequency modes are proportional to the Alfvén velocity. The magnetic fluctuations propagate in the diamagnetic direction of energetic ions. The comparison between the observed frequencies and shear Alfvén spectra calculated including the poloidal and toroidal mode couplings indicates that the high frequency modes exist inside the HAE gap near the plasma edge. In conclusion, the observed high frequency modes are related to the HAE localized near the edge and are destabilized via fundamental excitation. Detailed investigation of internal structure of these modes is left as an important future work.

The authors acknowledge the LHD technical group for their excellent operation of LHD. They also would like to thank Professor K. Matsuoka, Professor O. Motojima, Professor Y. Hamada, and Professor M. Fujiwara for their continuing encouragement. This work was supported in part by a Grant-in-Aid for Scientific Research from Japan Society for the Promotion of Science.

[1] K. L. Wong, Plasma Phys. Controlled Fusion **41**, R1 (1999).
[2] J. P. Goedbeloed *et al.*, Plasma Phys. Controlled Fusion **35**, B277 (1993).
[3] N. J. Fisch and J-R. Rax, Phys. Rev. Lett. **69**, 612 (1992).
[4] C. Z. Cheng and M. S. Chance, Phys. Fluids **29**, 3695 (1986).
[5] R. Betti and J. P. Freidberg, Phys. Fluids B **3**, 1865 (1991).
[6] M. Takechi *et al.*, Phys. Rev. Lett. **83**, 312 (2001).
[7] K. Toi *et al.*, Nucl. Fusion **40**, 1349 (2000).
[8] S. Yamamoto *et al.*, J. Plasma Fusion Res. **3**, 117 (2000).
[9] N. Nakajima, C. Z. Cheng, and M. Okamoto, Phys. Fluids B **4**, 1115 (1992).
[10] Ya. I. Kolesnichenko *et al.*, Phys. Plasmas **8**, 491 (2001).
[11] D. A. Spong, R, Sanchez, and A. Weller, Phys. Plasmas **10**, 3217 (2003).
[12] A. Iiyoshi *et al.*, Nucl. Fusion **39**, 1245 (1999).
[13] C. Beidler *et al.*, Fusion Technol. **17**, 148 (1990).
[14] M. C. Zarnstorff *et al.*, Plasma Phys. Controlled Fusion **43**, 237 (2001).
[15] S. Okamura *et al.*, Nucl. Fusion **41**, 1865 (2001).
[16] C. Schwab, Phys. Fluids B **5**, 3195 (1993).
[17] N. Nakajima, J. Plasma Fusion Res. **2**, 50 (1999).